Sensitivity and Frequency Coupling Indexes of Respiratory Sinus Arrhythmia in Response to Continuously Increasing and Decreasing Tidal Volume

Alejandra Guillén-Mandujano, Salvador Carrasco-Sosa

Universidad Autónoma Metropolitana-I, CDMX, México

Abstract

In 40 healthy subjects we compared the effects of chirped respiratory frequency (CRF) from 0.15 to 0.5 Hz combined with continuously increasing and decreasing tidal volume (V_T, 1.0-2.5-1.0 l) ($CRFV_T$) vs. those of the same CRF at fixed V_T (1.0 l) on the 45-s time-courses, estimated by a time-frequency distribution, of the central frequency and power of the high frequency components of RR ($_{CF}HF_{RR}$, $_{P}HF_{RR}$) and of respiration ($_{CF}HF_{RES}$, $_{P}HF_{RES}$), from which respiratory sinus arrhythmia (RSA) sensitivity (RSA_S) by alpha index, its coherence (RSA_{CO}), and the $_{CF}HF_{RR}$–$_{CF}HF_{RES}$ and RSA_S–$_{CF}HF_{RES}$ relations were computed. Compared to CRF, $CRFV_T$ caused: smaller ($p<0.04$) slope, intercept and correlation of RSA_S–$_{CF}HF_{RES}$ relation, with accentuation of the progressive reduction of RSA_S dynamics and smaller ($p<0.03$) means at 7.5, 15, 22.5 and 30s;smaller ($p<0.03$) 15, 22.5 and 30s means of RSA_{CO} dynamics; greater ($p<0.02$) intercept and smaller ($p<0.04$) slope of the $_{CF}HF_{RR}$–$_{CF}HF_{RES}$ relation, with greater ($p<0.01$) means at 7.5,15, 22.5 and 30s of $_{CF}HF_{RR}$ dynamics. Our findings support that increasing-decreasing V_T provokes an important depression of the RSA_S–$_{CF}HF_{RES}$ relation and a slight elevation on $_{CF}HF_{RR}$–$_{CF}HF_{RES}$ relation, suggesting a great reduction of the RSA gain driving mechanism and a slight enhancement of the frequency coupling one.

1. Introduction

The effect of increasing respiratory frequency (RF), applied either discontinuous or continuously, on respiratory sinus arrhythmia (RSA), indicated by the power of the high frequency component of R-R intervals ($_{P}HF_{RR}$), has been consistently described as a nonlinear inverse relationship between RF and $_{P}HF_{RR}$, analogous to that of a low-pass filter [1,2,3]. Most of the respiratory maneuvers used for obtaining this relation do not control the tidal volume (V_T) and, given their several minutes duration, provoke fatigue and hyperventilation in the subjects [1,2,3].

In HRV and RSA studies, the spectral analysis of the respiratory signal (RES) is not usually executed. In contrast, performing the spectral estimation of RES and R-R intervals (RR) time series via a time-frequency distribution (TFD) has allowed us to obtain the relationships between the power of the high-frequency component of respiration ($_{P}HF_{RES}$) and $_{P}HF_{RR}$ to compute RSA sensitivity (RSA_S) by alpha index, and between the central frequencies of $_{P}HF_{RES}$ ($_{CF}HF_{RES}$) and of $_{P}HF_{RR}$ ($_{CF}HF_{RR}$) to measure their coupling. With this method we have documented that continuously increased isometric exercise decreases RSA_S in proportion to its intensity [4] and that in response to the continuous increase of RF from 0.03 to 0.8 Hz, $_{CF}HF_{RR}$ only changed proportionally in the 0.18 to 0.45 Hz band [5].

How do V_T changes affect the RSA_S–$_{CF}HF_{RES}$ and $_{CF}HF_{RR}$–$_{CF}HF_{RES}$ relationships? To document this question, we devised an easy-to-perform respiratory maneuver in which RF and V_T vary simultaneously and linearly over wide ranges in a short period of time, to minimize the subjects' hyperventilation and fatigue. Thus, our objective was to compare, in healthy subjects, the effects provoked by the combination of continuously increasing-decreasing V_T with chirped RF ($CRFV_T$) to those of the same chirped RF at constant V_T (CRF) on the instantaneous 45-s time-courses of $_{CF}HF_{RR}$, $_{P}HF_{RR}$, $_{CF}HF_{RES}$ and $_{P}HF_{RES}$, estimated by a TFD, from which RSA_S, RSA coherence (RSA_{CO}), and the RSA_S–$_{CF}HF_{RES}$ and $_{CF}HF_{RR}$–$_{CF}HF_{RES}$ relations were computed.

2. Methods

2.1. Subjects

Forty healthy, normotensive and sedentary subjects, 21 men and 19 women, were studied. Mean age, height and weight were 23.5±1.5 years, 168±7 cm and 65.4±8.4 kg respectively. Their written informed consent was requested to participate. This study was approved by the ethics committee of our university.

 ISSN: 2325-887X DOI: 10.22489/CinC.2021.057

2.2. Protocol

Volunteers visited the laboratory twice. The first time, their health status and anthropometric variables were evaluated and they were trained to execute the breathing maneuvers correctly. In the second visit subjects performed, in sitting position, two breathing maneuvers in random order, with a 5-min resting period in between. Volunteers underwent: CRF, 15-s control, followed by 30 s of continuous and linear RF increase from 0.15 to 0.5 Hz at constant V_T of 1.0 l and $CRFV_T$, linearly increasing V_T from 1.0 to 2.5 l followed by linearly decreasing V_T to 1.0 l simultaneously with linearly increasing RF from 0.15 to 0.5 Hz. To provide guidance for the execution of the maneuvers, the target respiratory pattern and the RES signal were displayed on a screen. Subjects were instructed to match the pattern with their RES. ECG and RES were recorded throughout the protocol.

2.3. Signal recording and acquisition

ECG was detected at the CM5 bipolar lead using a bioelectric amplifier (Biopac). RES was obtained by integrating the flow signal (Validyne) provided by a pneumotachometer (Hans Rudolph). All signals were digitized at a sampling frequency of 1.0 kHz via an acquisition and display system (Biopac).

2.4. Data processing

R-wave peaks were detected to construct the R-R time series. RR and RES were cubic-spline interpolated, resampled at 8 Hz and detrended. Auto and cross time-frequency spectra of RR and RES were estimated with the smoothed pseudo-Wigner-Ville distribution. We extracted the instantaneous ${}_{P}HF_{RR}$, ${}_{CF}HF_{RR}$, ${}_{P}HF_{RES}$ and ${}_{CF}HF_{RES}$ from the first two-order moments of their TFD in the standard high-frequency band, from which we computed: RSA_S by alpha index (square root of the ${}_{P}HF_{RR}/{}_{P}HF_{RES}$ ratio), the coherence between ${}_{P}HF_{RR}$ and ${}_{P}HF_{RES}$, RSA_{CO}, the RSA_S–${}_{CF}HF_{RES}$ and ${}_{CF}HF_{RR}$–${}_{CF}HF_{RES}$ relations, and the difference between ${}_{CF}HF_{RES}$ and ${}_{CF}HF_{RR}$ ($\Delta_{CF}HF$). Maxima and minima of each RES cycle were detected to form the V_T and RF time series for their comparison with their equivalent spectral parameters. To highlight any patterned responses to the respiratory maneuvers in the time-courses, individual indexes dynamics were ensemble averaged. For statistical purposes, indexes dynamics were segmented into 7.5-s epochs.

2.5. Statistical analysis

Data were expressed as mean±SD. Mean values of individual indexes dynamics of each 7.5 s epoch were computed. Indexes dynamics were used to compute linear regressions and correlations subject by subject. Intra-maneuver epoch mean differences were tested by ANOVA for repeated measures. Post-hoc pairwise comparisons were performed by Tukey test. Inter-maneuver differences were tested by paired t-test. Statistical significance was accepted at $p<0.05$.

3. Results

The time domain RES indexes, RF and V_T time series, were strongly correlated with the spectral ones, ${}_{CF}HF_{RES}$ and ${}_{P}HF_{RES}$. The V_T-${}_{P}HF_{RES}$ relation presented a minimal non-significant hysteresis (Fig.1).

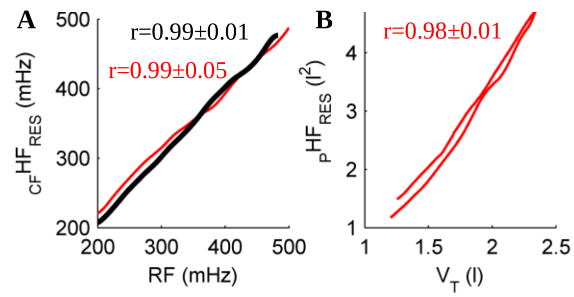

Fig.1. Ensemble averages of the individual relations between: A) RF time series and ${}_{CF}HF_{RES}$ dynamics; B) V_T time series vs. ${}_{P}HF_{RES}$ dynamics in CRF (black thick line) and $CRFV_T$ (red thin line).

The ensemble averages of ${}_{CF}HF_{RES}$ dynamics clearly depicted the continuous increase of RF from 0.15 to 0.5 Hz in both maneuvers, which did not show differences in any mean value (Fig. 2A). The ensemble averages of ${}_{P}HF_{RES}$ dynamics visibly described the continuous increase of V_T from 1.0 to 2.5 l followed by its reduction in $CRFV_T$ and the constant V_T of CRF, with differences in all their mean values comparisons (Fig. 2B).

The patterned responses of the spectral parameters dynamics provoked by the $CRFV_T$ maneuver, compared to that of CRF, were: accentuation of the progressive reduction of RSA_S dynamics which decreased, first rapidly from the onset until the third quarter of the maneuver, and then slowly, as shown by the smaller ($p<0.001$) mean values at 7.5, 15, 22.5 and 30s (Fig. 2C); the time-course of RSA_{CO} did not show differences until the second half of the maneuver but then it reduced progressively as shown by its smaller ($p<0.03$) mean values at 15, 22.5 and 30s (Fig. 2D); elevation of the progressive increment of the ${}_{CF}HF_{RR}$ dynamics, as shown by its greater ($p<0.001$) 7.5, 15, 22.5 and 30s means (Fig. 2E); depression of $\Delta_{CF}HF$ dynamics as documented by the smaller ($p<0.01$) 15 and 22.5s means (Fig. 2F); reduced ${}_{P}HF_{RR}$ dynamics that only showed differences until the end, with smaller ($p<0.01$) 30s mean value. The mostly non-different ${}_{P}HF_{RR}$ response contrasts with the important depression observed in the RSA_S dynamics (Fig. 2C).

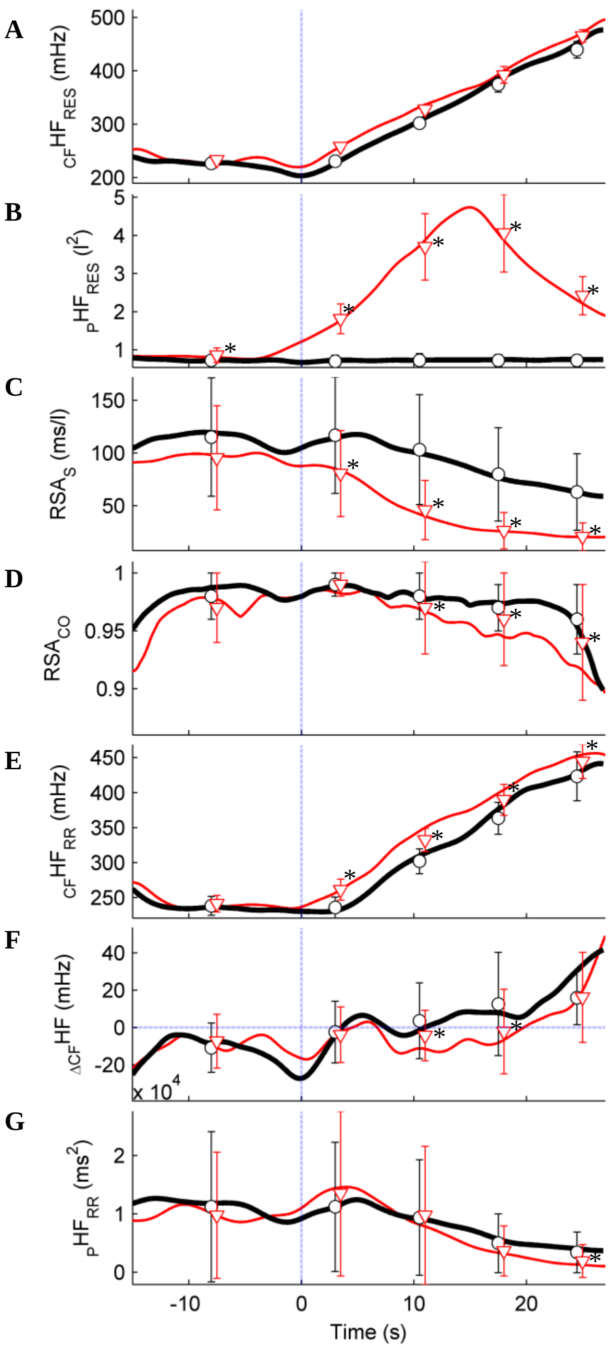

Fig. 2. Ensemble averages and mean±SD values of the individual time-courses of the spectral measures of RES, RR and RSA in CRF (black thick line) and $CRFV_T$ (red thin line) maneuvers. *p<0.03 $CRFV_T$ vs. CRF.

During CRF, the RSA_S–$_{CF}HF_{RES}$ relation showed very strong correlation (Fig. 3). $CRFV_T$ maneuver produced a great depression of the RSA_S–$_{CF}HF_{RES}$ relation associated with important reductions (p<0.04) of its correlation and intercept, and to a lesser degree, of its slope (Table 1, Fig. 3).

Table 1. Mean ± SD of the slopes and intercepts of the regressions of the relations of $_{CF}HF_{RES}$ with RSA_S and $_{CF}HF_{RR}$ in CRF and $CRFV_T$ maneuvers. N=40.

Relation	Condition	Slope	Intercept
RSA_S–	CRF	-0.41±0.22	254±110
$_{CF}HF_{RES}$	$CRFV_T$	-0.34±0.19*	184±98*
$_{CFE}HF_{RR}$–	CRF	0.85±0.18	49.8±62.5
$_{CF}HF_{RES}$	$CRFV_T$	0.79±0.19*	71.9±66.5*

*p<0.03 $CRFV_T$ vs. CRF.

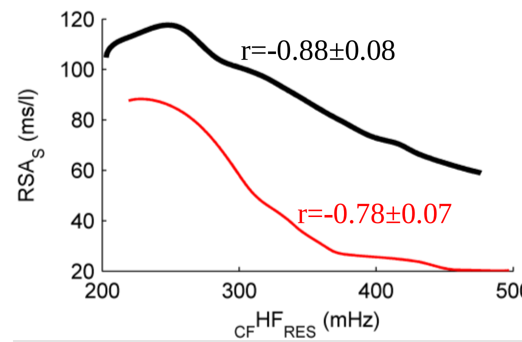

Fig. 3. Ensemble averages of the individual RSA_S-$_{CF}HF_{RES}$ relations in CRF (black thick line) and $CRFV_T$ (red thin line) conditions.

The correlations of the $_{CF}HF_{RR}$–$_{CF}HF_{RES}$ relation were very strong in both maneuvers (Fig. 4). $CRFV_T$ provoked a slight elevation of the $_{CF}HF_{RR}$–$_{CF}HF_{RES}$ relation, related to a greater intercept (p<0.02) and reduced slope (p<0.04) with no effect on the correlation (Table 1, Fig. 4).

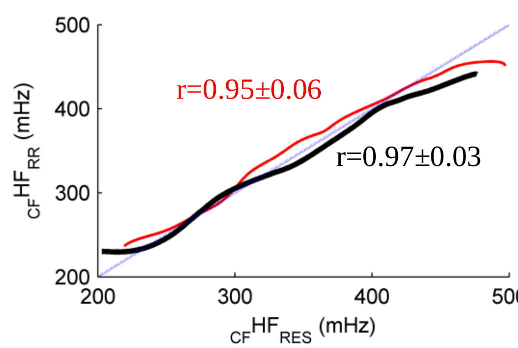

Fig. 4. Ensemble averages of individual $_{CF}HF_{RR}$-$_{CF}HF_{RES}$ relations in CRF (black line) and $CRFV_T$ (red line).

4. Discussion

With the aim of extending the knowledge of HRV, especially the understanding of RSA, we use the TFD-based spectral estimation of the time-courses of the high frequency powers ($_{P}HF$) and central frequencies ($_{CF}HF$) of the RES and RR time series, to compute RSA_S and RSA_{CO}, to obtain the RSA_S–$_{CF}HF_{RES}$ and $_{CF}HF_{RR}$–$_{CF}HF_{RES}$ relations. The changes in these relations are taken as indicators of the effects of the respiratory maneuvers. Our main findings are that $CRFV_T$ causes a marked depression in the RSA_S–$_{CF}HF_{RES}$ relation (Fig. 3), associated with a reduction of the RSA_{CO} dynamics (Fig. 2D), and a slight elevation of the $_{CF}HF_{RR}$–$_{CF}HF_{RES}$ relation (Fig. 4) associated with the $_{CF}HF_{RR}$ dynamics increase (Fig. 2E).

One of the basic knowledge that supports the functional mechanism of RSA is the inverse and non-linear relationship between RF and $_{P}HF_{RR}$ [1,2,3]. The RSA_S–$_{CF}HF_{RES}$ relationship is similar, but with a very strong linear correlation (Fig. 3), possibly because of the continuous, linear and short RF increment that we used and because RSA_S formalizes the normalization of $_{P}HF_{RR}$ by V_T in the frequency domain. Normalizing RSA amplitude by V_T through regression techniques in the time domain, improves its comparability [6].

We hypothesize that in the general mechanism of RSA, generated by the interaction of the respiratory pattern generating nuclei with the vagal nuclei [7], two dynamic interactive driving mechanisms participate: one for the frequency coupling, that allows $_{CF}HF_{RR}$ to closely follow RF changes, and the other for the gain, whose instantaneous level determines, at a constant respiratory input, the amplitude of $_{P}HF_{RR}$ changes. Possibly, these RSA mechanisms are associated to the open-close frequency and amplitude of the flow of the gate-like mechanism [8]. The functionality of the two proposed RSA mechanisms would be described by the $_{CF}HF_{RR}$–$_{CF}HF_{RES}$ and RSA_S–$_{CF}HF_{RES}$ relations.

$_{P}HF_{RES}$ and $_{CF}HF_{RES}$ can be considered surrogate variables of V_T and RF, as supported by the very strong correlation we found between them. However, using the RES spectral variables allow the uniform and coherent management in the frequency domain, i.e., computing RSA_S and RSA_{CO} time-courses.

The strong correlations found for the RSA_S–$_{CF}HF_{RES}$ and $_{CF}HF_{RR}$–$_{CF}HF_{RES}$ relations (Fig. 3 and Fig. 4) justify performing the statistical comparison between the slopes and intercepts of their linear regressions to assess the effect of $CRFV_T$. This maneuver provokes the reduction of the slope and the increase of the intercept of the $_{CF}HF_{RR}$–$_{CF}HF_{RES}$ relation, as well as the reduction of both in the RSA_S–$_{CF}HF_{RES}$ relation, but with greater effect on their intercepts (Table 1). In a previous study we reported the depression of the intercepts of the RSA_S–$_{CF}HF_{RES}$ and $_{CF}HF_{RR}$–$_{CF}HF_{RES}$ relations elicited by the active orthostatic test [5]. The marked depression of the RSA_S dynamics is associated with the decrease of RSA_{CO} time-course (Fig. 2 C, D), effect that suggests some uncoupling in the gain driving mechanism. Additionally**,** while all the epoch means of the time-course of RSA_S during $CRFV_T$ were significantly different than those of CRF (Fig. 2C), only one of $_{P}HF_{RR}$ was significantly different (Fig. 2E). This finding suggests that RSA_S outperforms $_{P}HF_{RR}$ as indicator. The increment elicited on the $_{CF}HF_{RR}$ dynamics (Fig. 2E), and the elevation of the $_{CF}HF_{RR}$–$_{CF}HF_{RES}$ relation (Fig. 4) are possibly associated to the enhancement of the frequency coupling mechanism.

To the best of our knowledge, this is the first study to report the utilization of a TFD on the RR and RES time series to obtain the RSA_S–$_{CF}HF_{RES}$ and $_{CF}HF_{RR}$–$_{CF}HF_{RES}$ relations, which showed that $CRFV_T$ provokes an important depression in the first relation and a slight increase in the second one.

The strong functional relationship between RF and $_{P}HF_{RR}$ [1,2,7] supports the suggestion that the spectral analysis of RES should be included as part of the spectral analysis of HRV, practice that could improve the physiological interpretation of $_{P}HF_{RR}$, now used together with $_{P}HF_{RES}$ for computing RSA_S, by indicating its mobility via $_{CF}HF_{RR}$, which is driven by $_{CF}HF_{RES.}$

In conclusion, our findings support that the 1.0-2.5-1.0l increasing-decreasing V_T provokes an important depression of RSA_S–$_{CF}HF_{RES}$ relation and a slight elevation of $_{CF}HF_{RR}$–$_{CF}HF_{RES}$ relation. Thus, the spectral estimation of the RR and RES time series via a TFD allows assessing the time-courses of $_{P}HF$ and $_{CF}HF$, as well as computing RSA_S, to form the RSA_S–$_{CF}HF_{RES}$ and $_{CF}HF_{RR}$–$_{CF}HF_{RES}$ relations, which can be used as functional indexes of the mechanisms that drive the gain and the frequency coupling of RSA.

References

[1] J. Saul, R. Berger, M. Chen, R. Cohen. "Transfer function analysis of autonomic regulation. II. Respiratory sinus arrhythmia". *Am. J. Physiol,*. vol. 256, pp. H153-H161, 1989.

[2] V. Novak, P. Novak, J. De Champlain, A. Le Blanc, et al. "Influence of respiration on heart rate and blood pressure fluctuations". *J. Appl. Physiol,*. vol. 74, pp. 617-626, 1993.

[3] J. Taylor, C. Myers, J. Halliwill, H. Seidel, D. Eckberg. "Sympathetic restraint of respiratory sinus arrhythmia: implications for vagal-cardiac tone assessment in humans". *Am. J. Physiol,*. vol. 280, pp. H2804-H2814, 2001.

[4] A. Guillén-Mandujano, S. Carrasco-Sosa. "Effects of two types of linearly increased isometric exercise on instantaneous baroreflex and respiratory sinus arrhythmia sensitivities computed by alpha index". *CinC,* vol. 45, 2018.

[5] A. Guillén-Mandujano, S. Carrasco-Sosa, P. Coello-Caballero "Frequency coupling and sensitivity spectral measures of the respiratory sinus arrhythmia system in response to increasing respiratory frequency". *CinC,* vol. 47, 2020.

[6] H. Kobayashi. "Normalization of respiratory sinus arrhythmia by factoring in tidal volume". *Appl. Human Sci.*, vol. 17, pp. 207-213, 1998.

[7] M. Elstad, E. O'Callaghan, A. Smith, et al. "Cardiorespiratory interactions in humans and animals: rhythms for life". *Am J Physiol* vol. 315, pp. H6-H17, 2018.

[8] D. Eckberg. "The human respiratory gate". *J. Physiol.,* vol. 548, pp. 339-352, 2003.

Address for correspondence:

Alejandra Guillén-Mandujano
Depto. Ciencias de la Salud, T-172. UAM-I, CDMX, México.
aguillen@izt.uam.com